Conformational Stability of the *Escherichia coli* HPr Protein: Test of the Linear Extrapolation Method and a Thermodynamic Characterization of Cold Denaturation†

Eric M. Nicholson‡ and J. Martin Scholtz*,‡,§

Departments of Biochemistry and Biophysics and of Medical Biochemistry and Genetics, Center for Macromolecular Design, Texas A&M University, College Station, Texas 77843

Received April 10, 1996; Revised Manuscript Received June 25, 1996⊗

ABSTRACT: The conformational stability of the histidine-containing phosphocarrier protein (HPr) from *Escherichia coli* has been determined using a combination of thermal unfolding and urea denaturation experiments. The analysis of the denaturation data provides a measure of the changes in conformational free energy, enthalpy, entropy, and heat capacity that accompany the equilibrium folding of HPr over a wide range of temperature and urea concentrations. In moderate concentrations of urea, HPr undergoes both high- and low-temperature unfolding, allowing for a reliable determination of the change in heat capacity for the conformational transition. The data are consistent with the linear free energy relationship commonly employed to analyze protein denaturation data, even over a relatively large temperature and urea concentration range. Furthermore, we find that a temperature-independent ΔC_p is adequate to describe HPr stability over the accessible temperature range. Finally, our data allow us to evaluate the energetics of the urea−protein interaction. For HPr, the changes in excess enthalpy and entropy of the denaturant−protein interaction(s) make only minor contributions to the observed ΔH and ΔS terms, presumably due in some part to the small size of the HPr protein.

A description of the mechanism of protein folding remains one of the most elusive problems of modern biochemistry. It has been over 30 years since we have realized that many small globular proteins can refold spontaneously without additional factors or assistance. One useful separation of the protein folding problem is into two components: one being the kinetic pathway for folding and the other being the thermodynamic factors that stabilize a particular protein fold over the unfolded forms. For many proteins, the equilibrium protein-folding reaction can be described adequately by a cooperative two-state transition, from folded protein to the unfolded or "random coil" form(s) of the polypeptide chain. This two-state approximation, however unrealistic on a molecular level, greatly simplifies the interpretation of thermodynamic protein stability data and provides a convenient way to determine the conformational stability of a protein, defined as the difference in Gibbs free energy between the two conformations of the polypeptide chain. The accurate determination of the thermodynamic stability of the folded form of a protein relative to the unfolded form(s), and the factors that contribute to the conformational stability, will greatly aid the protein structure prediction and design processes and will be a key component in the solution of the protein folding problem.

To assess the conformational stability of a protein, one must induce the equilibrium unfolding reaction and measure the populations of folded and unfolded forms. This is usually done by changing the temperature of the protein solution to induce a thermal unfolding transition or adding chemical denaturants such as aqueous guanidine hydrochloride or urea that cause most proteins to unfold. Regardless of the method used to induce the unfolding reaction, the data must be analyzed with a model for the folding transition to obtain a measure of the conformational stability of a protein. For most proteins that have been studied, the simple two-state model seems adequate to describe the equilibrium folding reaction and is in general use. Even if both unfolding reactions can be described by a two-state transition, there are some key differences between the two methods commonly employed to induce the reaction. In general, the analysis of thermal unfolding data will provide an estimate of the conformational stability of a protein at high temperatures, around the midpoint of the thermal unfolding transition, while the analysis of denaturant-induced unfolding data will provide a measure of the stability of a protein in a solution containing some amount of denaturant, generally greater that 1 or 2 M. In order to compare these two estimates of conformational stability, extrapolations to a common temperature and solution composition, for example 25 °C in water (or dilute buffer), must be made. These extrapolations are sometimes quite long, in terms of either temperature or denaturant concentration, and can lead to serious errors and inconsistencies when comparing estimates of conformational stability between the two methods.

The key parameter needed to extrapolate thermal unfolding data to any other temperature is the change in heat capacity (ΔC_p) for the folding reaction. This parameter provides the temperature dependence to the thermodynamic quantities ΔG, ΔH, and ΔS:

† This work was supported by a grant from the National Institutes of Health (R29-GM 52483). E.M.N. is supported by a predoctoral training fellowship from the National Institutes of Health (T32-GM 08523), and J.M.S. is the recipient of the American Cancer Society Junior Faculty Research Award (JFRA-577).

* Address correspondence to this author at the Department of Medical Biochemistry and Genetics, 440 Reynolds Medical Building, Texas A&M University Health Science Center, College Station, TX 77843-1114. Phone: (409) 845-0828. Fax: (409) 847-9481. E-mail: jm-scholtz@tamu.edu.

‡ Department of Biochemistry and Biophysics.

§ Department of Medical Biochemistry and Genetics.

⊗ Abstract published in *Advance ACS Abstracts,* August 15, 1996.

S0006-2960(96)00863-X CCC: $12.00

$$\Delta H(T) = \Delta H_g + \Delta C_p(T - T_g) \quad (1)$$

$$\Delta S(T) = \Delta S_g + \Delta C_p \ln(T/T_g) \quad (2)$$

$$\Delta G = \Delta H - T\Delta S \quad (3)$$

$$\Delta G(T) = \Delta H_g\left(1 - \frac{T}{T_g}\right) + \Delta C_p[T - T_g - T\ln(T/T_g)] \quad (4)$$

Here we have adopted the nomenclature of Schellman (Becktel & Schellman, 1987; Chen & Schellman, 1989; Schellman, 1987, 1994) with the subscript indicating the parameter at a reference temperature, T_g, where $\Delta G = 0$.

For solvent denaturation curves, the key parameter is the *m* value, defined as the gradient of the change in folding free energy with molar denaturant concentration ($\partial\Delta G/\partial$[denaturant]):

$$\Delta G' = \Delta G - m[\text{urea}] \quad (5)$$

The primes on the parameters, T_g', $\Delta G'$, and $\Delta H'$, are the values determined in the presence of the indicated amount of urea. According to the linear free energy model (Chen & Schellman, 1989; Schellman, 1994), changes in Gibbs free energy, enthalpy, entropy, and heat capacity that occur on protein unfolding all have a linear dependence on the molar concentration of denaturant, [urea] in this case:

$$\Delta H' = \Delta H - h[\text{urea}] \quad (6)$$

$$\Delta S' = \Delta S - s[\text{urea}] \quad (7)$$

$$\Delta C_p' = \Delta C_p - c[\text{urea}] \quad (8)$$

For the urea−protein interaction, it is possible to express the free energy term, *m*, in terms of the enthaply, entropy, and heat capacity changes such that

$$m = h - Ts + c[(T - T_g) - T\ln(T/T_g)] \quad (9)$$

The parameters, ΔC_p and *m*, are clearly orthogonal, with ΔC_p giving us a way to determine conformational free energy at every temperature in the absence of denaturant and *m* providing a means of calculating the conformational free energy at any concentration of denaturant, including the limit of no denaturant, at a given temperature. Equation 9 illustrates that *m* should be temperature-dependent. One important aspect of the present study is to determine if we can indeed observe the expected temperature dependence and to attempt to quantify the thermodynamic parameters provided by eq 9.

The inability of the analyses of the data derived from thermal unfolding and solvent denaturation experiments to sometimes provide an identical estimate of the conformational free energy of a protein at a particular set of conditions may therefore result from errors in either ΔC_p, *m*, or the temperature dependence to the denaturant−protein interaction provided by *h*, *s*, or *c*. If, on the other hand, it could be demonstrated that ΔC_p and *m* for a protein are independent of the concentration of the denaturant and temperature, or if the temperature and denaturant dependencies to ΔC_p and *m* are known, the orthogonality of the two types of unfolding experiments could be exploited to generate a free energy unfolding surface for a protein as functions of both denaturant concentration and temperature. This is the approach employed here for the HPr protein using a simple spectroscopic probe to monitor the unfolding transition.

HPr is a small globular protein with no disulfide bonds or other prosthetic groups. HPr serves as a phosphocarrier protein in the phosphoenolpyruvate-dependent carbohydrate transport system (PTS) in both Gram-negative and Gram-positive bacteria [reviewed by Meadow et al. (1990)]. In addition, the PTS regulates a variety of cellular processes through inducer exclusion, inducer expulsion, and catabolite repression in many bacteria (Postma et al., 1993). The three-dimensional structures of HPr from a variety of bacterial sources have been determined by crystallographic [*Bacillus subtilis* (Herzberg et al., 1992), *Escherichia coli* (Jia et al., 1993b), and *Streptococcus faecalis* (Jia et al., 1993a, 1994b)] and NMR techniques [*B. subtilis* (Wittekind et al., 1992), *E. coli* (Klevit & Waygood, 1986; Hammen et al., 1991; van Nuland et al., 1992, 1994), and *Staphylococcus aureus* (Kalbitzer et al., 1991; Kalbitzer & Hengstenberg, 1993)]. The proteins from these sources show identical folding topologies with two or three α-helices on one face of a four-stranded, antiparallel β-sheet [for reviews, see Herzberg and Klevit (1994) and Jia et al. (1994a)].

Here we describe the complete stability surface, the dependence of the Gibbs energy of folding on temperature and urea concentration, for the histidine-containing phosphocarrier protein (HPr) from *E. coli* (*ec*HPr).[1] In generating this surface, we provide a direct test of the linear free energy relationship for protein thermodynamics and gain insight into the thermodynamics of the HPr−urea interaction.

MATERIALS AND METHODS

The expression and purification of *ec*HPr was performed as described by Anderson et al. (1991). The *E. coli* strain (TP2811), the plasmid containing the wild-type *E. coli* HPr gene, and protein for initial studies were generous gifts of Professor E. Bruce Waygood. In our hands, the protein yield was greater than 100 mg of homogeneous HPr from 6 L of late logarithmic cells. Protein purity was judged to be greater than 95% by denaturing gel electrophoresis and analytical isoelectric focusing.

Circular dichroism at 222 nm was used to monitor the equilibrium unfolding transition using an Aviv 62DS spectropolarimeter equipped with a temperature control and stirring unit. The thermal unfolding curves were performed with heating rates from 30 to 90 °C/h in cuvettes with path lengths of 1, 5, or 10 mm. The reversibility of the thermal transition was determined in each case by monitoring the return of the CD signal at 222 nm upon cooling from 90 to 10 °C immediately after the conclusion of the thermal transition. In all cases, the transitions were independent of heating rate, ≥95% reversible, and independent of protein concentration. Some reversibility was lost upon prolonged exposure of the sample to high temperatures, particularly in the presence of urea. This loss of reversibility is presumably due to chemical modification of the protein by the products of urea decomposition.

For the urea denaturation curves at a constant temperature, the urea solutions were prepared fresh daily in buffered solutions containing 10 mM potassium phosphate (K/P_i) at

[1] Abbreviations: LEM, linear extrapolation method; *ec*HPr, the HPr protein from *Escherichia coli;* CD, circular dichroism spectroscopy.

pH 7.0. The concentration of the urea stock solution was determined by refractive index measurements (Pace, 1986). Since the folding equilibrium was reached rapidly for *ec*HPr, the urea denaturation curves were performed using the method of serial additions of urea to a protein sample with a correction made for the increase in volume (Scholtz, 1995). The additions of small aliquots of concentrated urea in buffer are made directly to the protein sample in the cuvette, allowing the sample to reach thermal and chemical equilibrium before recording the CD signal.

Best-fit parameters and their confidence intervals expressed as one standard deviation are given for each fit. For the analysis of a transition curve with well-defined baselines, a modification of the linear extrapolation method (LEM) of Santoro and Bolen (1988) was used, using the curve-fitting methods in the KaleidaGraph software (Synergy Software, PCS Inc.). A single urea denaturation, where the observed CD signal at each point in the unfolding experiment is m^{o}_{obs}, can be analyzed with the equation

$$m^{o}_{obs} = [N_0 + a_N[\text{urea}] + (D_0 + a_D[\text{urea}]) \times \exp[m/RT([\text{urea}]-C_{mid})]]/\left[1 + \exp\left[\frac{m}{RT}([\text{urea}]-C_{mid})\right]\right] \quad (10)$$

with N_0, a_N, D_0, a_D, m, and C_{mid} as parameters. This expression combines the LEM, eq 5 where $\Delta G_{water} = mC_{mid}$, the two-state assumption for the unfolding reaction, and linear pre- and post-transition baselines, $X_0 + a_x[\text{urea}]$. An example of the nonlinear least-squares fit of eq 10 to a typical urea denaturation experiment is shown as the solid curve in Figure 1B.

To facilitate comparison of urea denaturation data and thermal denaturation data, both types of data must be converted to the fraction of native protein (f_N) as a function of either [urea] or temperature. For the urea denaturation data, we find

$$f_N = \frac{m^{o}_{obs} - D_0 - a_D[\text{urea}]}{N_0 + a_N[\text{urea}] - D_0 - a_D[\text{urea}]} \quad (11)$$

An analogous expression for the thermal unfolding data can be obtained by substituting T for [urea] in eq 11. These expressions assume linear pre- and post-transition baselines. For the data in the transition regions of the unfolding curves ($0.05 < f_N < 0.95$), the two-state model ($f_N + f_D = 1$) was employed to calculate an equilibrium constant and Gibbs energy of folding at each point:

$$K_{eq} = \frac{f_D}{f_N} = \frac{1 - f_N}{f_N} \quad (12)$$

$$\Delta G(T,[\text{urea}]) = -RT \ln K_{eq} \quad (13)$$

RESULTS

The conformational stability of HPr at pH 7.0 has been determined using a combination of thermal unfolding in the presence of urea or by urea denaturation at various temperatures. Typical unfolding experiments, as monitored by the change in mean residue ellipticity at 222 nm by CD, $[q]_{222}$, are shown in Figure 1. In each of these denaturation experiments, the lines indicate the pre- and post-transition regions of the curves. For a single urea denaturation curve (Figure 1B), eq 10 can be used to find the best-fit values for the six parameters needed to describe the transition. The solid curve through the data in Figure 1B shows the results of this analysis, providing C_{mid} and m as shown in Table 1.

Representative thermal unfolding experiments, normalized to the fraction of native conformation (f_N) with eq 11, are shown in Figure 2. The high-temperature transition occurs at lower temperatures as the concentration of urea is increased. Low-temperature unfolding, or cold denaturation,

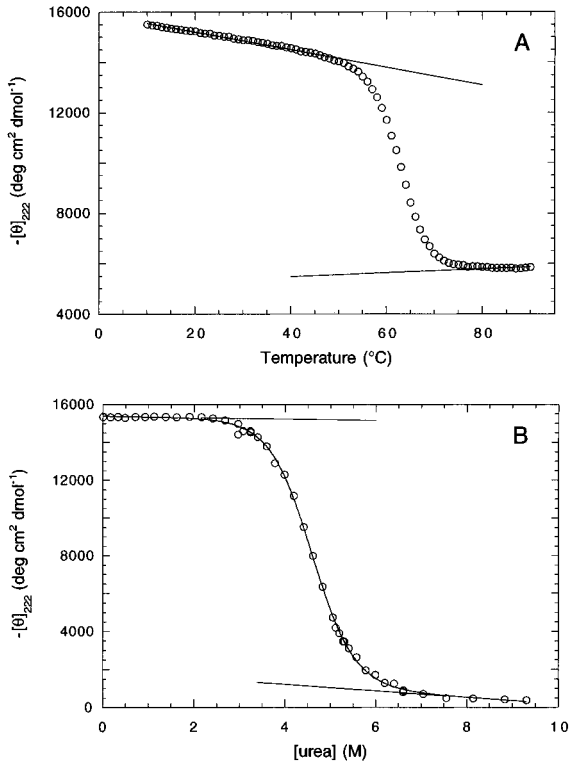

FIGURE 1: Thermal (A) and urea-induced (B) unfolding transitions for *ec*HPr as monitored by CD at 222 nm illustrating the pre- and post-transition baselines for each experiment. The thermal unfolding curve was in aqueous buffer only (10 mM K/P_i, pH 7.0), while the urea denaturation curve was in the same buffer, plus the indicated amount of urea, at 15 °C. The curve through the transition region of the urea denaturation curve was generated with eq 10, and the corresponding best-fit parameters are given in Table 1.

Table 1: Analysis of the Urea Denaturation Curves at Different Temperatures[a]

temperature (°C)	C_{mid} (M urea)	m value (kcal mol^{-1} M^{-1})	ΔG_{water} (kcal mol^{-1})
0	4.00 ± 0.09	1.29 ± 0.14	4.63 ± 0.10
5	4.38 ± 0.05	1.18 ± 0.05	5.08 ± 0.05
10	4.58 ± 0.04	1.36 ± 0.05	5.31 ± 0.05
15	4.66 ± 0.12	1.20 ± 0.05	5.41 ± 0.14
20	4.70 ± 0.02	1.24 ± 0.07	5.46 ± 0.05
25	4.58 ± 0.04	1.19 ± 0.06	5.31 ± 0.07
30	4.32 ± 0.05	1.14 ± 0.05	5.00 ± 0.05
35	4.04 ± 0.03	1.01 ± 0.05	4.68 ± 0.05
40	3.58 ± 0.06	1.06 ± 0.05	4.14 ± 0.08
45	2.90 ± 0.05	1.01 ± 0.06	3.37 ± 0.05
50	2.09 ± 0.18	1.11 ± 0.08	2.42 ± 0.22

[a] The data in the transition regions of the urea denaturation curves were analyzed with the linear extrapolation model provided by eq 5 using a modification of the method of Santoro and Bolen (1988) as shown in eq 10. ΔG_{water} values are determined using the indicated C_{mid} value and the average m value; $\langle m \rangle = 1.16 \pm 0.11$ kcal mol^{-1} M^{-1}.

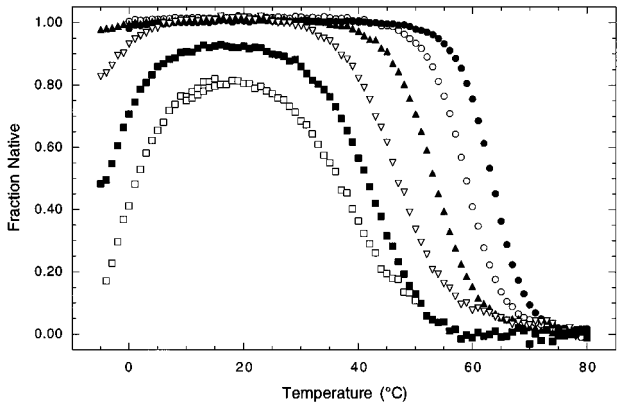

FIGURE 2: Thermal unfolding curves for *ec*HPr in various urea concentrations at pH 7.0 (10 mM K/P_i) as monitored by the change in ellipticity at 222 nm converted to fraction folded as described in the text. The error on any single point is smaller than the size of the symbol. The urea concentration in each is 0 M (●), 1 M (○), 2 M (▲), 3 M (▽), 3.5 M (■), and 4 M (□).

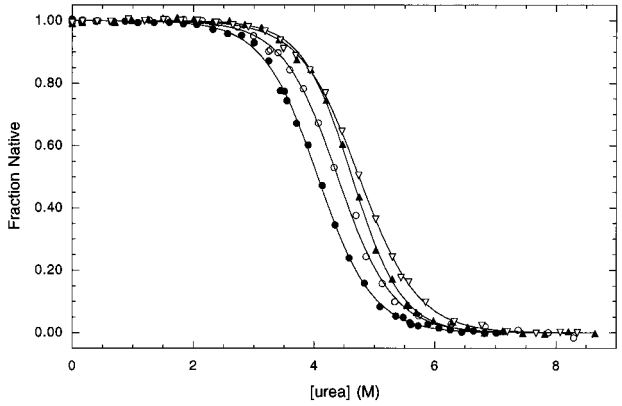

FIGURE 3: Representative urea unfolding curves for *ec*HPr at various temperatures (10 mM K/P_i, pH 7.0) as monitored by the change in ellipticity at 222 nm converted to fraction folded as described in the text. The error on any single point is smaller than the size of the symbol. The temperature for each is 0 °C (●), 5 °C (○), 10 °C (▲), and 15 °C (▽). The curves through the data represent the fit of eq 10 to each data set, providing the best-fit parameters given in Table 1.

is clearly evident at urea concentrations above 3 M. All transitions are fully reversible as shown by the return of the CD signal at 222 nm after cooling the protein from 90 to 10 °C, provided that the protein solution is not allowed to remain at temperatures greater than 70 °C for more than 1 h. Upon prolonged exposure to high temperatures, particularly in the presence of urea, some reversibility is lost, presumably due to irreversible aggregation or modification of the protein by urea decomposition products (data not shown). We do not see any evidence for hysteresis or alterations in the thermal unfolding curves with changes in scan rate, scanning from low to high or high to low temperatures, changing protein concentration, or repeated scans of the same protein sample.

Several representative urea denaturation experiments at constant temperature are shown in Figure 3. These transitions are also fully reversible and independent of protein concentration and reach equilibrium rapidly. The rapid folding or unfolding reaction allows us to use the simple "titration method" for performing our urea denaturation experiments (see Materials and Methods). Cold denaturation is suggested here, as seen by the decrease in the midpoint of the cooperative unfolding transition as the temperature is lowered. The results of the analyses of these curves, using

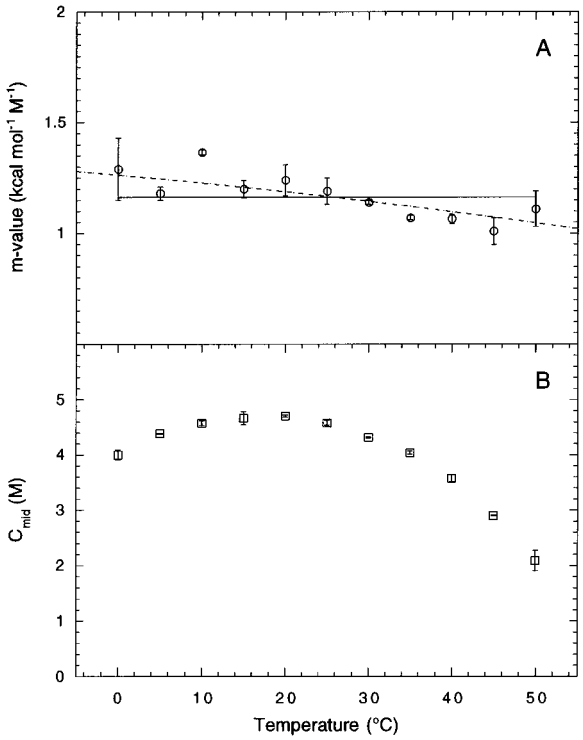

FIGURE 4: Effects of temperature on the best-fit *m* values (A) and C_{mid} (B) for the urea denaturation curves at 11 different temperatures. The error bars represent the larger of the standard error or the uncertainty in repeated measurements of each parameter. The solid line in panel A represents the mean of the *m* values when treated as temperature-independent, 1.16 ± 0.10 kcal mol^{-1} M^{-1}. The dashed curve shows the calculated temperature dependence to *m* resulting from the global analysis of the data using eq 18 (see the text for details).

the LEM as described in Materials and Methods, are shown in Table 1 and Figure 4. We find that the *m* values show very little temperature dependence over the entire 50 °C range of temperatures with an average value of 1.16 ± 0.11 kcal mol^{-1} M^{-1} (Figure 4A, solid line). The slight temperature dependence and the dashed line are discussed below. Figure 4 also shows the best-fit C_{mid} values at each temperature.

Conformational Stability of ecHPr. Using the data shown in Figure 2 for thermally induced unfolding in the presence of various concentrations of urea, together with eqs 12 and 13, we have calculated the conformational stability of *ec*HPr for every point in each transition region. These are shown in Figure 5 (open symbols). We have also used the urea denaturation data (Figure 3, Table 1) to determine the conformational stability as functions of temperature and [urea]. These are also shown in Figure 5 (filled symbols). There are several important observations about Figure 5. (1) The coincidence of the two data sets provides evidence for the validity of our use of the optical baselines/plane for the native and unfolded forms of the protein (see above). (2) The agreement between the data sets indicates that each point in Figure 5 represents a true equilibrium measurement of the conformational stability of *ec*HPr. (3) *ec*HPr exhibits both high- and low-temperature unfolding. As the concentration of urea is increased, the high-temperature unfolding transition occurs at lower temperatures, while the low-temperature unfolding transition occurs at higher temperatures. (4) Using this combination of data, we can determine the conformational stability of *ec*HPr over a very wide

Table 2: Thermodynamic Parameters for Thermal Unfolding of *ec*HPr at pH 7.0[a]

[urea]	T_g'	$T_g'^c$	$\Delta H_g'$	$\Delta H_g'^c$	$\Delta S_g'$	$\Delta S_g'^c$	$\Delta C_p'$	T_h'	T_s'	$\Delta G_s'$
0.0	336.6	244.6	75.8	−61.3	225	−251	1.49	285.7	289.4	5.45
1.0	331.7	248.5	64.8	−53.5	195	−215	1.42	286.1	289.1	4.26
2.0	326.7	255.0	54.5	−46.4	167	−182	1.40	287.8	290.0	3.12
3.0	320.6	261.8	41.2	−36.0	129	−138	1.31	289.2	290.6	1.96
4.0	310.2	274.5	28.0	−25.8	90	−94	1.27	288.2	288.9	0.97

[a] $\Delta H_g'$ and $\Delta S_g'$ are calculated at T_g', the midpoint of the high-temperature unfolding transition, and $\Delta H_g'^c$ and $\Delta S_g'^c$ are calculated at $T_g'^c$, the temperature midpoint for the cold denaturation reaction. $\Delta C_p'$, T_g', and $T_g'^c$ were calculated from the stability curves (Figure 5) as described in the text. $\Delta C_p'$ and $\Delta C_p'^c$ are identical for both the high- and low-temperature unfolding reactions, so only one value is shown. T_h', T_s', and $\Delta G_s'$ were determined as described in the text. The concentration of urea is expressed as molar. All temperatures are in Kelvin. ΔH and ΔG are in kilocalories per mole. ΔS is in calories per mole per Kelvin. ΔC_p is in kilocalories per mole per Kelvin. The errors on the temperatures are ±0.1−0.4 K, ΔH ±1.2−2.7 kcal mol^{-1}, ΔS ±10−30 cal mol^{-1} K^{-1}, ΔC_p ±0.05−0.15 kcal mol^{-1} K^{-1}, and $\Delta G_s'$ ±0.05−0.14 kcal mol^{-1} as determined from least-squares analysis. The specific error on each parameter is indicated in the text or in other figure legends.

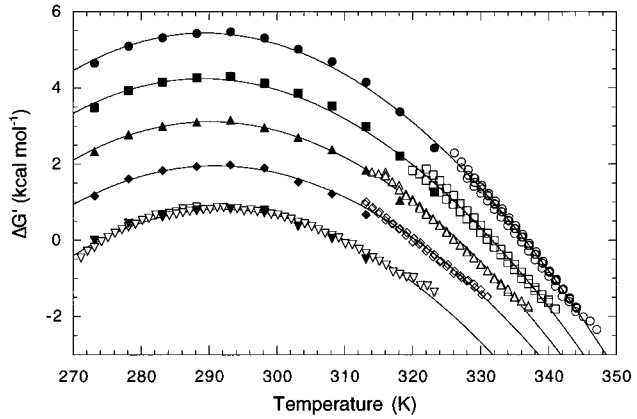

FIGURE 5: Variation of the observed conformational free energy of folding as a function of temperature and urea concentration for every point in each transition regions of the urea and thermal denaturation experiments. From top to bottom, the urea concentration is 0 M (●, ○), 1 M (■, □), 2 M (▲, △), 3 M (◆, ◇), and 4 M (▼, ▽). The solid symbols are the extrapolations of the urea denaturation data at the indicated temperature, and the open symbols represent data from the transition regions of the thermal unfolding experiments. The curves through the data points represent the fit of eq 4 to each data set and provide estimates for the cardinal thermodynamic parameters shown in Table 2.

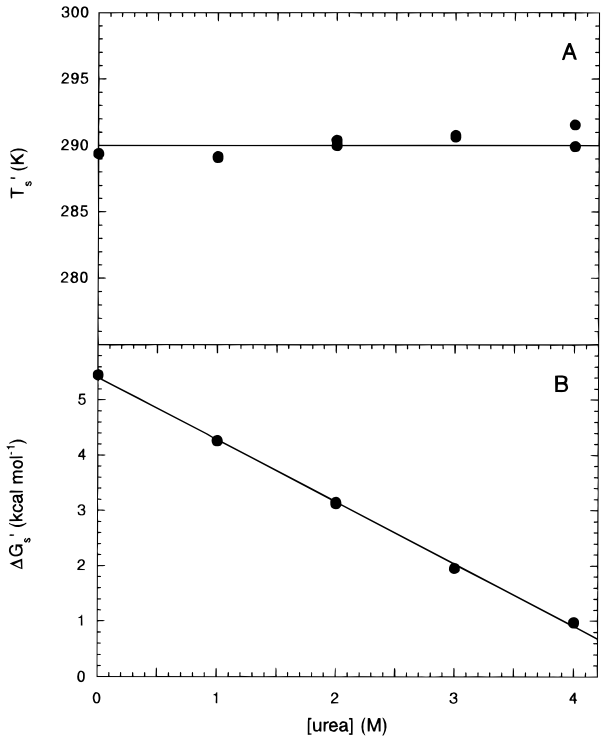

FIGURE 6: Dependence on the molar urea concentration for the best-fit values for T_s' (A) and $\Delta G_s'$ (B). The errors are smaller than the size of the symbols. The line in panel A represents the average T_s of 290.0 ± 0.8 K (16.9 °C) over the entire range of urea concentrations. The slope of the line in panel B is 1.13 ± 0.06 kcal mol^{-1} M^{-1}, and the *y* intercept is 5.41 ± 0.09 kcal mol^{-1}, the maximum conformational stability of *ec*HPr in the absence of urea.

temperature range, from −2 to 74 °C. This allows us to determine the temperature dependence of the thermodynamic parameters over a large temperature range. (5) The variation of the observed conformational stability ranges from ca. −2 to +5.5 kcal mol^{-1}, allowing us to determine the urea and temperature dependence of the thermodynamic parameters.

We have analyzed each of the stability curves shown in Figure 5 with a modification of the Gibbs−Helmholtz relationship given in eq 4. This provides estimates of $\Delta H_g'$, T_g', $\Delta S_g'$, and $\Delta C_p'$ at each concentration of urea. The results of the fit of eq 4 to the data are shown as curves in Figure 5, and the thermodynamic parameters are collected in Table 2. The thermodynamic parameters describing the cold denaturation transition were also determined with eq 4 with the constraint that $\Delta H_g' < 0$. The best-fit parameters, $\Delta H_g'^c$, $T_g'^c$, and $\Delta S_g'^c$, where the superscript c indicates the cold denaturation process, are also shown in Table 2. The best-fit value for $\Delta C_p'$ is identical for both the high- and low-temperature unfolding transitions, as expected from the constant ΔC_p model (see below).

The temperature dependence of the free energy of unfolding, denoted in the stability curve by Becktel and Schellman (1987), has some other notable features, such as a temperature of maximum stability T_s and the conformational stability evaluated at that temperature ΔG_s. These quantities can be determined for each of the five curves shown in Figure 5 using

$$\ln\left(\frac{T_g'}{T_s'}\right) = \frac{\Delta H_g'}{T_g'\Delta C_p'} \quad (14)$$

$$T_h' = T_g' - \frac{\Delta H_g'}{\Delta C_p'} \quad (15)$$

$$\Delta G_s' = \Delta C_p'(T_s' - T_h') \quad (16)$$

Table 2 also lists $\Delta G_s'$ and T_s' values for each of the curves, as evaluated from the data in Table 2 and eqs 14−16. Figure 6 shows the dependence on the molar urea concentration for T_s' and $\Delta G_s'$. For T_s', there is very little variation with the concentration of urea and the average value is 16.9 ± 0.8 °C. For $\Delta G_s'$, the dependence on the urea concentration is

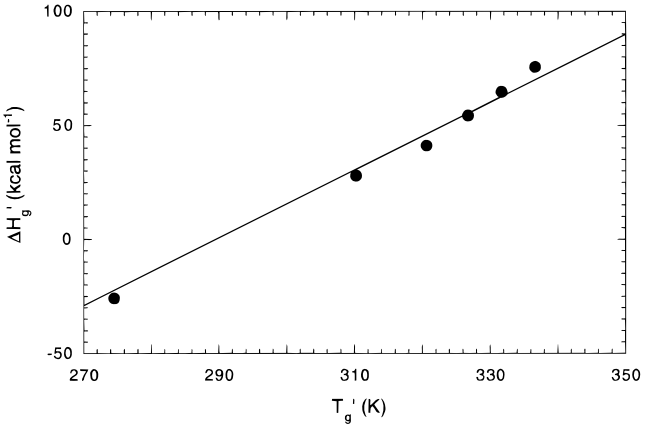

FIGURE 7: Relationship between $\Delta H_g'$ and T_g' determined from the analyses of all the high-temperature unfolding transitions and the single low-temperature transition that occurs above 0 °C (the 4 M urea data set) as shown in Figure 4. The slope of this line provides an estimate of the apparent ΔC_p (1.49 ± 0.09 kcal mol^{-1} K^{-1}) for *ec*HPr stability. The errors are approximately the size of the symbols.

linear, as expected for the LEM (eq 5), and the slope, or *m*, is 1.13 ± 0.06 kcal mol^{-1} M^{-1}, in good agreement with the average of the urea denaturation curves shown in Table 1. The *y* intercept of Figure 6B is ΔG_s, the maximum stability of *ec*HPr in the absence of denaturant (5.41 ± 0.09 kcal mol^{-1}).

The data in Table 2 can be used to determine other relationships between the thermodynamic parameters. In Figure 7, we show the relationship between $\Delta H_g'$ and T_g' determined from the analyses of all the high-temperature unfolding transitions and the single low-temperature transition that occurs above 0 °C (the 4 M urea data set) shown in Figure 4. T_g' therefore spans a 62 °C range in temperature, while $\Delta H_g'$ covers a range of over 100 kcal mol^{-1}. The data are described well by a straight line, with a slope, or apparent $\Delta C_p'$, of 1.49 ± 0.09 kcal mol^{-1} K^{-1}. As stated, this is only an apparent ΔC_p value, because contributions to $\Delta H_g'$ from the interaction of *ec*HPr with urea have not been removed (see below). Nonetheless, this apparent ΔC_p is nearly identical to our best estimate for the true ΔC_p for *ec*HPr (1.42 ± 0.09 kcal mol^{-1} K^{-1}, see below).

Evaluation of the Thermodynamics of the ecHPr−Urea Interaction. The data shown in the five stability curves in Figure 5 can also be used to analyze the urea dependence of the thermodynamic parameters as a test of the linear free energy model (eqs 5−8). For all concentrations of urea, $\Delta H'$, $\Delta S'$, and $\Delta G'$ can be evaluated at any temperature using eqs 1−4 in conjunction with the values for $\Delta H_g'$, $\Delta S_g'$, T_g', and $\Delta C_p'$ shown in Table 2. We have calculated each of these parameters at several temperatures between 0 and 60 °C to verify the linear relationship between the thermodynamic parameters and the molar concentration of urea. Figure 8 displays these data and confirms the linear model described by eqs 5−8 for each thermodynamic parameter $\Delta H'$, $\Delta S'$, $\Delta G'$, and $\Delta C_p'$ over the entire range of urea concentrations and temperatures. The slopes of these plots provide the effects of urea on the given parameter, *h*, *s*, *m*, and *c*, respectively. The changes in $\Delta H'$ and $\Delta S'$ with urea concentration do show a temperature dependence, as expected, while the temperature dependence of *m* is much smaller, due in part to entropy−enthalpy compensation of the *ec*HPr−urea interaction.

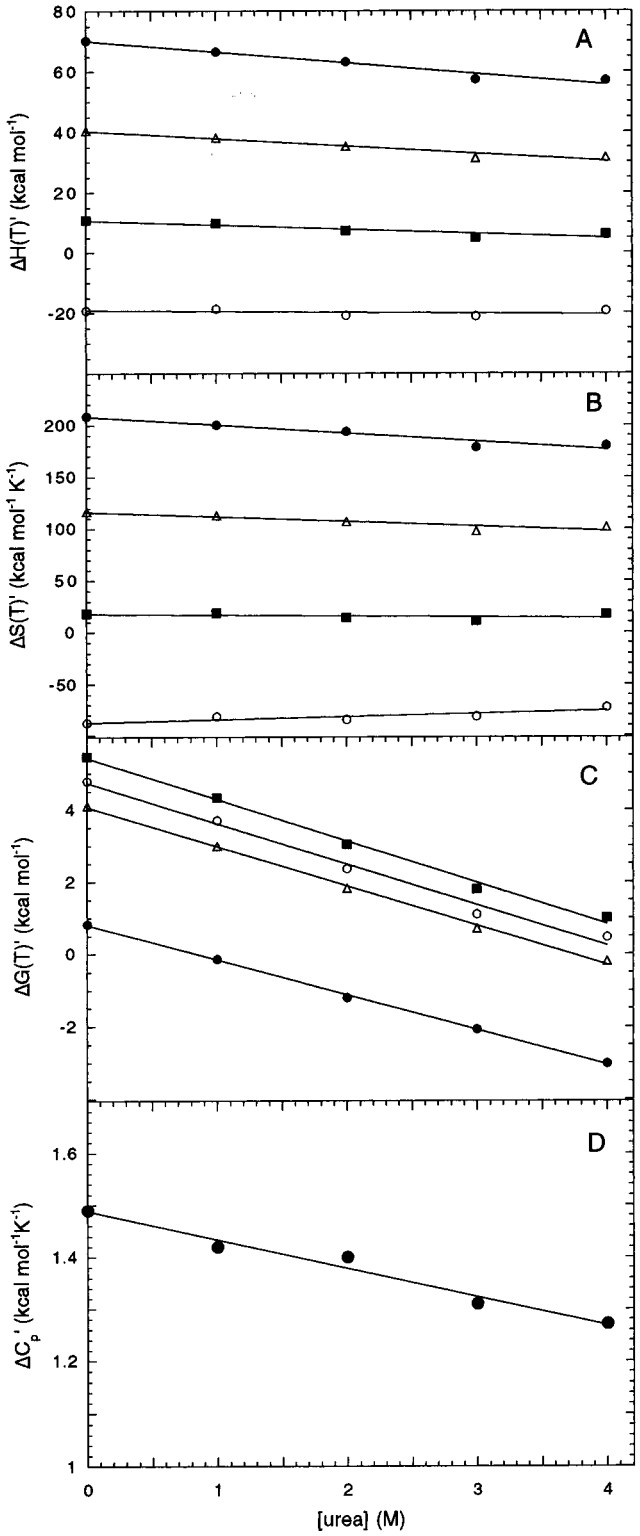

FIGURE 8: Urea dependence of the cardinal thermodynamic parameters $\Delta H(T)'$ (A), $\Delta S(T)'$ (B), $\Delta G(T)'$ (C), and $\Delta C_p'$ (D). For panels A−C, the temperatures are 333 K (●), 313 K (△), 293 K (■), and 273 K (○). For each temperature, the line represents a linear fit to the data, in accordance with the LEM. For ΔC_p in panel D, the slope of the line, *c*, is 50 ± 20 cal mol^{-1} K^{-1} M^{-1}. See the text for further analysis.

Figure 8 also shows the urea dependence of $\Delta C_p'$ as determined from the analyses of the stability curves shown in Figure 5. There is a change in $\Delta C_p'$ which appears to be linear with the molar concentration of urea, in accordance

Table 3: Thermodynamic Parameters for the Folding of *ec*HPr at pH 7.0

parameter[a]	global analysis I[b]	global analysis II[c]
ΔC_p (kcal mol^{-1} K^{-1})	1.45 ± 0.08	1.42 ± 0.09
ΔH_g (kcal mol^{-1})	70.8 ± 3.4	69.8 ± 3.4
ΔS_g (cal mol^{-1} K^{-1})	210 ± 13	209 ± 10
T_g (°C)	63.8 ± 0.5	63.1 ± 0.4
m (kcal mol^{-1} M^{-1})	1.13 ± 0.04	−
h (kcal mol^{-1} M^{-1})	−	2.9 ± 1.3
s (cal mol^{-1} K^{-1} M^{-1})	−	55 ± 40
c (cal mol^{-1} K^{-1} M^{-1})	−	40 ± 35
(variance)$^{1/2}$	0.24	0.22

[a] The variable or fixed parameter in eq 17 or 18 is listed along with the associated units. ΔS_g is determined from the ratio of ΔH_g and T_g. The last entry represents the square root of the variance of the nonlinear least-squares fit. [b] The global analysis of all the data (642 points) in the transition regions for both the thermal and urea denaturation curves was analyzed with eq 17. The errors represent the 67% confidence intervals provided by the nonlinear least-squares analysis. [c] The global analysis of all the data (642 points) in the transition regions for both the thermal and urea denaturation curves was analyzed with eq 18 with h, s, and c allowed to vary, providing the temperature dependence to m as shown in eq 9. The errors represent the 67% confidence intervals provided by the nonlinear least-squares analysis.

with eq 8. Fitting eq 8 to the data provides $\Delta C_p = 1.48 \pm 0.06$ kcal mol^{-1} and $c = 50 \pm 20$ cal mol^{-1} K^{-1} M^{-1}. The small urea dependence suggests that $\Delta C_p'$ does decrease upon increasing the urea concentration. This observation, along with the evaluations of h and s described above, provides direct evidence for the validity of the linear free energy model.

Global Analysis of Urea and Thermal Denaturation Data for ecHPr. Since we have demonstrated that the linear free energy model does appear to hold for the unfolding of *ec*HPr with temperature and urea, and we have suitable forms for the urea and temperature dependence of the thermodynamic parameters, we have performed a "global analysis" of the entire data set represented by each of the thermal unfolding curves and urea denaturation curves. In total, we have used 642 points, representing $\Delta G(T,[\text{urea}])$ for each point in the transition regions of the unfolding curves. These data were used as input for a nonlinear least-squares analysis to

$$\Delta G(T,[\text{urea}]) = \Delta H_g\left(1 - \frac{T}{T_g}\right) + \Delta C_p[T - T_g - T\ln(T/T_g)] - m[\text{urea}] \quad (17)$$

and for the case where m is temperature-dependent to

$$\Delta G(T,[\text{urea}]) = \Delta H_g\left(1 - \frac{T}{T_g}\right) + \Delta C_p[T - T_g - T \times \ln (T/T_g)] - [h - Ts + c[T - T_g - T\ln(T/T_g)]][\text{urea}] \quad (18)$$

The results of these analyses are shown in Table 3. By comparison of the square root of the variance of the fits, it is clear that including a temperature dependence of m does improve the fit slightly. The best-fit values for h, s, and c were used to calculate the temperature dependence of m using eq 9. These results are shown as the dashed line in Figure 4A. A key aspect of the global analyses of the data using eq 17 or 18 is that the cardinal parameters governing the protein unfolding reaction do not vary, regardless of which of the two equations is fit to the data. The best-fit values for all the parameters are also identical, within error, to those found by independent analyses of individual unfolding curves (Table 1) or groups of curves (Table 2). This excellent agreement provides evidence in support of the applicability of the linear free energy model for the thermodynamics of *ec*HPr folding.

DISCUSSION

A complete description of the conformational stability of a protein as a function of temperature represents the stability curve (Becktel & Schellman, 1987). This complete description allows one to calculate the stability of a protein at any temperature using the Gibbs−Helmholtz relationship (eq 4). Here we provide a description of the stability curve for *ec*HPr using a combination of thermal- and urea-induced unfolding. Our data also allow us to quantify the energetics of the *ec*HPr−urea interaction. There are three principal observations from our results. (1) In moderate concentrations of urea, HPr exhibits cold denaturation, and thus, both high- and low-temperature unfolding can be observed in the accessible temperature range. (2) The data are consistent with a temperature-independent ΔC_p over the large temperature range of the unfolding transitions. (3) The simple two-dimensional analysis, using urea and temperature as protein unfolding agents, supports the use of the linear free energy model for the thermodynamic stability of *ec*HPr.

Two-State Analysis of ecHPr Folding. Our probe for monitoring the unfolding transition is the change in the far-UV CD signal as the protein unfolds. The analysis of thermal- or urea-induced unfolding data is then made with the two-state assumption for the reaction. Key to our analysis is the observation that the unfolding curves are reversible and superimposable for either unfolding or refolding, showing no hysteresis using either perturbant of the transition. Furthermore, the unfolding curves are independent of protein concentration and, for the thermal unfolding experiments, independent of scan rate. One assumption implicit in our analysis is that the denatured state(s), either at high temperatures in the absence or urea or at lower temperatures at high urea concentrations, can be treated as thermodynamically indistinguishable, even though our spectroscopic probe for the transition gives different values for the unfolded states. Our results indicate that we can indeed treat these differences in spectroscopic measures of the unfolded state(s) as simple optical differences and therefore can apply the appropriate post-transition baseline to determine the fraction of native protein (see Materials and Methods). The coincidence of calculated $\Delta G(T,[\text{urea}])$ points in Figure 5, derived from independent evaluations of urea denaturation curves and thermal denaturation curves, supports the use of our data analysis protocols. This is a key point. Since we are looking for variations in the observed ΔG values with temperature and/or [urea], it is important that we have confidence in the methods used to calculate $\Delta G(T,[\text{urea}])$.

There are several other cases where thermally unfolded proteins give optical signals different than those of the same protein in the presence of high concentrations of denaturants (Pace & Tanford, 1968; Robertson & Baldwin, 1991; Scholtz, 1995; Agashe & Udgaonkar, 1995). It has been shown that, in many of these cases, these two unfolded states can be represented adequately as a single thermodynamic state (Pfiel

& Privalov, 1976; Privalov, 1979). That is, the thermodynamic stability of the folded state of a protein relative to the unfolded state(s) is independent of the perturbant used to induce the unfolding transition. Therefore, the differences in optical properties of the two denatured forms of a protein can be treated as simple baseline effects, as we have done here.

The two-state model for protein folding is in widespread use as it is a convenient model to use for the equilibrium unfolding transition. Verification of the two-state model is difficult; however, several lines of evidence suggest that *ec*HPr unfolding, either by the addition of urea or by an increase in temperature, adheres to the two-state model. For the thermal unfolding reaction, an isodichroic point is observed in the far-UV CD spectra obtained through the transition region (data not shown), consistent with the two-state model. Furthermore, the good agreement between $\Delta G(T,[\text{urea}])$ values through the transition regions of either thermal- or urea-induced unfolding curves is also consistent with the two-state model. Also, the changes in conformational stability brought about by a site-specific mutation of *ec*HPr are identical when comparing thermal, and urea-induced unfolding (Hammen et al., 1995; Thaper et al., 1996). Finally, we have preliminary differential scanning calorimetry (DSC) data that provide identical measures of ΔH_{cal} and ΔH_{vH}, suggesting the two-state model is providing a good representation of the thermal unfolding data (E. M. Nicholson and J. M. Scholtz, unpublished data). Furthermore, the enthalpy change and midpoint of the DSC endotherm are identical, within error, to those found in the present study, using CD to monitor the unfolding transition. All the data we have to this point suggest that the two-state model provides a reasonable description of the equilibrium folding−refolding transition for *ec*HPr.

Stability Curve and Cold Denaturation of ecHPr. The stability curve of a protein is defined as the variation of the conformational free energy of folding with temperature (Becktel & Schellman, 1987). In order to evaluate this function (eq 4), ΔH_g, T_g, and ΔC_p must be known. In general, a single thermal unfolding curve, monitored either with an optical probe or with DSC, is not of sufficient accuracy to provide reliable estimates of all three parameters, with ΔC_p being the most difficult to obtain. In order to provide a wider range in variability of ΔH_g and T_g, necessary to determine ΔC_p (eq 1), the unfolding transition must be shifted to other temperature regions. This is done by changing the composition of the solvent, either by changes in pH or by the addition of a second protein stability perturbant, in this case urea. This obviously introduces a new variable that needs to be determined (the *m* value, eq 5). For the cases where changes in pH are used to move the transition region to other temperatures, corrections must also be made for potential ionization enthalpy differences between protein groups and the buffers. In most cases, this is achieved by a judicious choice of buffers such that the ionization enthalpies of the protein groups and buffers match. However, using different buffers to change the pH of the solution introduces the possibility of differential interactions between buffers and the protein with unknown effects on the energetic consequences of these potential interactions. Here we have elected to use one buffer and pH and use urea as a way to alter the transition region for the thermal unfolding transition. This provides an opportunity for us to evaluate the energetics of the urea−protein interaction and compare these results with the large body of data on denaturant−protein and denaturant−peptide energetics (Nozaki & Tanford, 1963, 1970; Robinson & Jencks, 1965; Nandi & Robinson, 1984; Makhatadze & Privalov, 1992; Agashe & Udgaonkar, 1995).

In moderate concentrations of urea, *ec*HPr undergoes cold denaturation (Figure 5). The process of cold denaturation has been observed for many proteins over the years (Christensen, 1952; Brandts, 1964; Pace & Tanford, 1968; Privalov et al., 1986; Chen & Schellman, 1989; Scholtz, 1995; Agashe & Udgaonkar, 1995) and is a result of the simple relationship described by eq 4 with $\Delta C_p > 0$ for protein unfolding. The appearance of cold denaturation is strong support for the applicability of eq 4 for the thermodynamics of protein stability. The cold denaturation exhibited by *ec*HPr is interesting not only because it allows the complete stability curve to be obtained but also because it allows unfolding data to be collected over a much wider range of protein stability. Together, the stability curves determined here (Figure 5) cover a temperature range greater than 70 °C. The unfolding free energy change covers a range of over 7 kcal mol^{-1}, and the curvature of the stability curve, which is directly related to ΔC_p, can be easily observed. Our results indicate that ΔC_p for *ec*HPr appears to be temperature-independent, even over this extended temperature range. Recently, it has been demonstrated that ΔC_p should not be treated as temperature-independent (Privalov & Makhatadze, 1990). This is obviously true as the laws of thermodynamics state that ΔC_p must vanish at 0 K. The question really is one of the range of temperatures we are able to investigate and the magnitude of the temperature dependence of ΔC_p. The temperature dependence of ΔC_p has recently been parameterized in terms of changes in accessible surface area during the unfolding reaction and other structural parameters (Gómez et al., 1995). We have used this approach to estimate the potential temperature dependence of ΔC_p for *ec*HPr by calculating the changes in solvent accessible surface area from the crystal structure of *ec*HPr (Jia et al., 1993b) and the denatured state (using an extended conformation for the polypeptide backbone). Using the equations given by Gómez and co-workers (1995) along with the calculated changes in accessible surface area on folding, we find $\Delta C_p(T)$ for *ec*HPr can be described by $\Delta C_p(T) = 1.4 + 0.02T - 0.0003T^2$ kcal mol^{-1} K^{-1}, with T expressed in degrees Celsius. The calculated ΔC_p is 1.4 kcal mol^{-1} K^{-1} near 0 and 75 °C, reaching a maximum near 40 °C of 1.7 kcal mol^{-1} K^{-1}. The best estimate of ΔC_p from our data, when treated as temperature-independent, is 1.42 ± 0.09 kcal mol^{-1} K^{-1}, in excellent agreement with the values predicted near the temperature midpoints for our high- and low-temperature unfolding transitions. In addition, when we include the temperature dependence of ΔC_p as described above, the fits of eqs 17 or 18 to our data do not change the values of the cardinal parameters, or the overall variance of the fit, from those shown in Table 3. So, while we cannot say definitively that ΔC_p is temperature-independent over the range of our data, it appears that a constant ΔC_p is adequate to describe our data.

Why does *ec*HPr exhibit cold denaturation? The answer is revealed in the values of the cardinal thermodynamic parameters. First, the temperature of maximum stability, T_s, for the proteins is well above 0 °C, the practical lower limit

for protein stability studies in aqueous solution at normal pressures (Figure 6A). Second, the maximum conformation stability, denoted ΔG_s in the nomenclature of Becktel and Schellman (1987), is quite modest for *ec*HPr (see Figure 6B). These criteria are necessary, but not sufficient, to observe cold denaturation. The final criterion is the ratio of $\Delta H/\Delta C_p$. For *ec*HPr, ΔH at 25 °C is 16.4 kcal mol^{-1}, a value somewhat smaller than those observed for many proteins, which range from 25 to 75 kcal mol^{-1} (Privalov, 1979). Three other proteins that exhibit cold denaturation, myoglobin (Privalov et al., 1986), barstar (Agashe & Udgaonkar, 1995), and a monomeric version of λ repressor (Huang & Oas, 1996), also have low values for ΔH at 25 °C: 7.8, 4, and 6 kcal mol^{-1}, respectively. Furthermore, when ΔC_p values are compared, *ec*HPr, myoglobin, barstar, and monomeric λ repressor all have some of the highest ΔC_p values, on a per residue basis, 16−18 cal mol^{-1} K^{-1} residue^{-1}. Therefore, these four proteins have unusually low values of $\Delta H/\Delta C_p$, the final criterion for observable cold denaturation.

Thermodynamics of the Urea−ecHPr Interaction. With the approach we have utilized to determine the conformational stability of *ec*HPr, we have used a combination of urea and thermal unfolding experiments. These data cover a wide temperature range in solutions from 0 to 4 M urea. These data allow us to investigate the thermodynamics of the interaction of urea with *ec*HPr and to provide a test of the linear free energy model for protein−denaturant interactions. The use of the linear free energy model has a long history, first being used empirically by Greene and Pace (1974) and later given a theoretical explanation by Schellman and colleagues (Schellman, 1987, 1990, 1994; Chen & Schellman, 1989; Schellman & Gassner, 1996). An alternative model, called the binding model, has also been used to investigate the thermodynamics of protein−denaturant interactions, most recently by Makhatadze and Privalov (1992). The basic premise of either model is that denaturant interacts more strongly with the unfolded form of a protein. The main experimental distinction between the two models is the predicted dependence on denaturant concentration. The LEM predicts a linear change in ΔG with molar denaturant concentration, while the binding model predicts a logarithmic dependence. For weak-binding systems, like the urea−protein interaction, the distinction between these models is not as clear [see Scholtz et al. (1995) for a discussion; Schellman & Gassner, 1996]. Our data seem totally consistent with the simple linear model, not only for ΔG but also for ΔH, ΔS, and ΔC_p (Figure 8); however, we cannot rule out the possibility that the binding or solvent exchange models might be a better way to interpret our data. Since the LEM is in widespread use, especially for the analysis of urea denaturation curves, we have elected to apply this method to analyze our data.

There are some interesting aspects of the data represented in Figure 8. The first is that $\Delta H'$ (Figure 8A) and $\Delta S'$ (Figure 8B) change very little with urea, that is h and s in eqs 6 and 7 are small compared to ΔH and ΔS for the protein conformational change. At 298 K, the enthalpy of the urea−*ec*HPr interaction is only −2 kcal mol^{-1} at 1 M urea. For comparison, Makhatadze and Privalov (1992) found that the enthalpy of the interaction between urea and ribonuclease A or lysozyme is approximately −8 to −10 kcal mol^{-1} at 298 K and 1 M urea. This indicates that urea interacts less favorably with *ec*HPr than with ribonuclease A or lysozyme, possibly due to the smaller size of the HPr protein. In a recent study on another small protein, Agashe and Udgaonkar (1995) also found that the enthalpy of the interaction between guanidinium chloride (GdmCl) and another small protein, barstar, is also much smaller than with ribonuclease A or lysozyme. This may be a general feature of small proteins; the small size provides fewer interaction sites for denaturants like urea or GdmCl with a concomitant smaller contribution to the observed thermodynamic parameters. This observation also explains the results shown in Figure 6; perturbation of T_g' and $\Delta H_g'$ with urea provides a reasonable estimate of ΔC_p for *ec*HPr, without having to correct for the contribution of the enthalpy of the urea−protein interaction, since the latter contribution is small. For most proteins, it is necessary to correct the observed enthalpy changes for solvent−protein heat effects to obtain a reliable measure of ΔC_p for the protein conformational change [however, see Liu and Sturtevant (1996)]. The generality of our results for other small proteins is currently under investigation.

We also find that ΔC_p shows a slight decrease with increasing concentrations of urea (Figure 8D). It is well-established that ΔC_p is related to changes in water accessible surface area upon protein unfolding (Spolar et al., 1992; Murphy & Freire, 1992; Myers et al., 1995; Gómez et al., 1995), with changes in nonpolar surface area contributing in a positive sense to ΔC_p and changes in polar surface area decreasing the magnitude of ΔC_p for protein unfolding. If we apply these observations to our data, where ΔC_p decreases as the urea concentration is increased, one must conclude that the nature of the denatured state, or the relative contributions of the solvent accessibility of polar and nonpolar groups, is changing as we introduce more urea into the solution. More work is needed to confirm this observation for other proteins and model compounds.

Conclusions. We have characterized the equilibrium unfolding of *ec*HPr and have determined the two-dimensional conformational stability surface for the protein as a function of both temperature and the concentration of urea. The data are described well by the simple linear model for the effects of denaturants on stability not only for changes in the Gibbs free energy of folding but also for the enthalpy, entropy, and heat capacity changes that accompany the conformational transition. For this protein, the contributions that the urea−protein interactions make to the observed values for ΔH and ΔS are small, presumably due in part to the small size of the HPr protein. The HPr protein also exhibits cold denaturation, and thus, both high- and low-temperature unfolding can be used to determine the cardinal thermodynamic parameters governing the conformational stability of *ec*HPr.

ACKNOWLEDGMENT

We thank Rachel Klevit and Bruce Waygood for generous gifts of purified protein for the initial studies and Terry Oas, Nick Pace, Andy Robertson, John Schellman, and members of the Pace and Scholtz groups for helpful discussions. We also acknowledge the helpful suggestions of a reviewer.

REFERENCES

Agashe, V. R., & Udgaonkar, J. B. (1995) *Biochemistry 34*, 3286−3299.

Anderson, J. W., Bhanot, P., Georges, F., Klevit, R. E., & Waygood, E. B. (1991) *Biochemistry 30*, 9601−9607.

Becktel, W. J., & Schellman, J. A. (1987) *Biopolymers 26*, 1859−1877.
Brandts, J. F. (1964) *J. Am. Chem. Soc. 86*, 4291−4301.
Chen, B., & Schellman, J. A. (1989) *Biochemistry 28*, 685−691.
Christensen, L. K. (1952) *C. R. Trav. Lab. Carlsberg, Ser. Chim. 28*, 37−169.
Gómez, J., Hilser, V. J., Xie, D., & Freire, E. (1995) *Proetins: Struct., Funct. Genet. 22*, 404−412.
Greene, R. F., & Pace, C. N. (1974) *J. Biol. Chem. 249*, 5388−5393.
Hammen, P. K., Waygood, E. B., & Klevit, R. E. (1991) *Biochemistry 30*, 11842−11850.
Hammen, P. K., Scholtz, J. M., Anderson, J. W., Waygood, E. B., & Klevit, R. E. (1995) *Protein Sci. 4*, 936−944.
Herzberg, O., & Klevit, R. (1994) *Curr. Opin. Struct. Biol. 4*, 814−822.
Herzberg, O., Reddy, P., Sutrina, S., Saier, M., Reizer, J., & Kapadia, G. (1992) *Proc. Natl. Acad. Sci. U. S. A. 89*, 2499−2503.
Huang, G. S., & Oas, T. G. (1996) *Biochemistry 35*, 6173−6180.
Jia, Z., Vandonselaar, M., Quail, J. W., & Delbaere, L. T. J. (1993a) *Nature 361*, 94−97.
Jia, Z., Quail, J. W., Waygood, E. B., & Delbaere, L. T. J. (1993b) *J. Biol. Chem. 268*, 22490−226501.
Jia, Z., Quail, J. W., Delbaere, L. T. J., & Waygood, E. B. (1994a) *Biochem. Cell Biol. 72*, 202−217.
Jia, Z., Vandonselaar, M., Hengstenberg, W., Quail, J. W., & Delbaere, L. T. J. (1994b) *J. Mol. Biol. 236*, 1341−1355.
Kalbitzer, H. R., & Hengstenberg, W. (1993) *Eur. J. Biochem. 216*, 205−214.
Kalbitzer, H. R., Neidig, K.-P., & Hengstenberg, W. (1991) *Biochemistry 30*, 11186−11192.
Klevit, R. E., & Waygood, E. B. (1986) *Biochemistry 25*, 7774−7781.
Liu, Y., & Sturtevant, J. M. (1996) *Biochemistry 35*, 3059−3062.
Makhatadze, G. I., & Privalov, P. L. (1992) *J. Mol. Biol. 226*, 491−505.
Meadow, N. D., Fox, D. K., & Roseman, S. (1990) *Annu. Rev. Biochem. 59*, 497−542.
Murphy, K. P., & Freire, E. (1992) *Adv. Protein Chem. 43*, 313−361.
Myers, J. K., Pace, C. N., & Scholtz, J. M. (1995) *Protein Sci. 4*, 2138−2148.
Nandi, P. K., & Robinson, D. R. (1984) *Biochemistry 23*, 6661−6668.
Nozaki, Y., & Tanford, C. (1963) *J. Biol. Chem. 238*, 4074−4081.
Nozaki, Y., & Tanford, C. (1970) *J. Biol. Chem. 245*, 1648−1652.
Pace, C. N. (1986) *Methods Enzymol. 131*, 266−280.
Pace, C. N., & Tanford, C. (1968) *Biochemistry 7*, 198−208.
Pfiel, W., & Privalov, P. L. (1976) *Biophys. Chem. 4*, 33−40.
Postma, P. W., Lengeler, J. W., & Jacobson, G. R. (1993) *Microbiol. Rev. 57*, 543−594.
Privalov, P. L. (1979) *Adv. Protein Chem. 33*, 167−241.
Privalov, P. L., & Makhatadze, G. I. (1990) *J. Mol. Biol. 213*, 385−391.
Privalov, P. L., Griko, Y. V., Venyaminov, S. Y., & Kutyshenko, V. P. (1986) *J. Mol. Biol. 190*, 487−498.
Robertson, A. D., & Baldwin, R. L. (1991) *Biochemistry 30*, 9907−9914.
Robinson, D. R., & Jencks, W. P. (1965) *J. Am. Chem. Soc. 87*, 2462−2470.
Santoro, M. M., & Bolen, D. W. (1988) *Biochemistry 27*, 8063−8068.
Schellman, J. A. (1987) *Biopolymers 26*, 549−559.
Schellman, J. A. (1990) *Biophys. Chem. 37*, 121−140.
Schellman, J. A. (1994) *Biopolymers 34*, 1015−1026.
Schellman, J. A., & Gassner, N. C. (1996) *Biophys. Chem. 59*, 259−275.
Scholtz, J. M. (1995) *Protein Sci. 4*, 35−43.
Scholtz, J. M., Barrick, D., York, E. J., Stewart, J. M., & Baldwin, R. L. (1995) *Proc. Natl. Acad. Sci. U.S.A. 92*, 185−189.
Spolar, R. S., Livingstone, J. R., & Record, M. T., Jr. (1992) *Biochemistry 31*, 3947−3955.
Thaper, R., Nicholson, E. M., Waygood, E. B., Scholtz, J. M., & Klevit, R. E. (1996) *Biochemistry 35*, 10339−10346.
van Nuland, N. A. J., Grötzinger, J., Dijkstra, K., Scheek, R. M., & Robillard, G. T. (1992) *Eur. J. Biochem. 210*, 881−891.
van Nuland, N. A. J., Hangyi, I. W., van Schaik, R. C., Berendsen, H. J. C., van Gunsteren, W. F., Scheek, R. M., & Robillard, G. T. (1994) *J. Mol. Biol. 237*, 554−559.
Wittekind, M., Rajagopal, P., Branchini, B. R., Reizer, J., Saier, M. H., Jr., & Klevit, R. E. (1992) *Protein Sci. 1*, 1363−1376.

BI960863Y